Design and Simulation of GaSb/InAs 2D Transmission-Enhanced Tunneling FETs

Pengyu Long, Evan Wilson, Jun Z. Huang, *Member, IEEE*, Gerhard Klimeck, *Fellow, IEEE*, Mark J. W. Rodwell, *Fellow, IEEE*, and Michael Povolotskyi, *Member, IEEE*

***Abstract*— We describe the design of double-gate InAs/GaSb tunneling field-effect transistors (TFETs) using GaSb electron wave reflector(s) in the InAs channel. The reflections from the source p-n junction and from the reflector(s) add destructively, causing the net transmission to approach unity at certain energies. The energy range of transmission enhancement can be broadened by the appropriate placement of multiple barriers. With 10^{-3} A/m OFF-current (I_{OFF}) and a 0.3 V power supply, the subthreshold swing is improved from 14.4 to 4.6 mV/decade and the ON-current (I_{ON}) is improved from 35 to 96 A/m, compared with a conventional GaSb/InAs TFET.**

***Index Terms*— TFETs, heterojunctions.**

I. Introduction

POWER dissipation seriously constrains VLSI performance [1]. Low switching energy requires a low power supply voltage, yet decreased standby power requires either increased voltages or reduced transistor subthreshold swing (*S.S.*). In conventional MOSFETs, thermal carrier injection limits the *S.S.* to 60mV/dec. [1]. Though tunnel FETs (TFETs) [2]–[4] can obtain smaller *S.S.,* their on-current (I_{ON}) is limited by low PN junction tunneling probability [3]. The tunneling probability is limited by the effective mass and tunneling distance across the PN tunnel junction. For nanoscale TFETs, quantization increases the barrier energy and carrier effective masses, decreasing the tunneling probability. The tunneling distance is limited by source doping, channel thickness and gate dielectric, and hence is not easily reduced [5]. Although use of InAs-GaSb heterojunctions reduces the tunneling barrier energy and tunneling distance, under strong quantization in channels of a few nm thickness, the barrier energies and tunneling distances remain significant, hence the tunneling probabilities and on-currents remain small. Alternative methods to increase I_{on} of TFETs are needed.

Manuscript received September 18, 2015; revised October 22, 2015; accepted November 2, 2015. Date of publication November 4, 2015; date of current version December 24, 2015. This work was supported by the U.S. National Science Foundation NEB program. This material is based upon work supported by the National Science Foundation under Grant 1125017. NEMO5 developments were critically supported by an NSF Peta-Apps award OCI-0749140 and by Intel Corporation. The review of this letter was arranged by Editor S. J. Koester.

P. Long, E. Wilson, J. Z. Huang, G. Klimeck, and M. Povolotskyi are with the Network for Computational Nanotechnology and Birck Nanotechnology Center, Purdue University, West Lafayette, IN 47907 USA (e-mail: davidlong180@gmail.com).

M. J. W. Rodwell is with the Department of Electrical and Computer Engineering, University of California at Santa Barbara, Santa Barbara, CA 93106-9560 USA.

Color versions of one or more of the figures in this letter are available online at http://ieeexplore.ieee.org.

Digital Object Identifier 10.1109/LED.2015.2497666

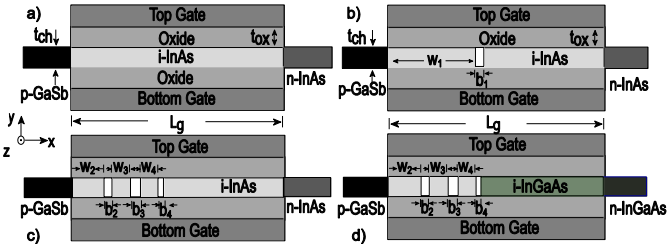

Fig. 1. Cross-sections of a) no-barrier, b) one-barrier, c) three-barrier InAs-channel, and d) three-barrier InGaAs-channel designs. The barriers b_{1-4}, are GaSb.

Avci and Young proposed a TFET with a reversed (p-InAs/n-GaSb) heterojunction [6], introducing a second barrier and a resonant bound state. Current increases sharply as the resonant state is aligned in energy with the Fermi window. Though *S.S.* is improved, the maximum I_{ON} remains low as the resonant state is narrow in energy. Here we show that embedding multiple barriers into the channel can broaden the energy range of transmission enhancement, significantly improving I_{ON}.

II. Device Design

The proposed transmission-enhanced TFETs are PN tunnel FETs with one or several phase-shift and electron-reflector layers. Reflections of the electron wave from the reflector layers (Fig. 2b) interfere destructively with reflections from the PN tunnel barrier, reducing the electron reflection probability, thus increasing the transmission probability. To increase I_{ON}, the transmission probability is increased over a broad energy range. The designs are based on a p-GaSb/n-InAs double-gate TFET, (design 1, Fig. 1a). The channel thickness is t_{ch}, the gate oxide has thickness t_{ox} and dielectric constant $\varepsilon_{r,ox}$. The gate length is L_g, and source and drain doping density are N_S and N_D. Transport is along the [100] direction. The channel is two-dimensional, extending in the z direction (perpendicular to the page). In designs 2 and 3 (Fig. 1b, c) the channel contains one or three GaSb barriers. The well and barrier widths, w and b, set the resonant state energies and barrier reflectivities. In design 4 (Fig. 1d), the channel and drain material is replaced by an InGaAs alloy. Table 1 gives parameters.

III. Simulation Method and Results

Devices are simulated using the atomistic nanoelectronics modeling software NEMO5 [7], which solves self-consistently

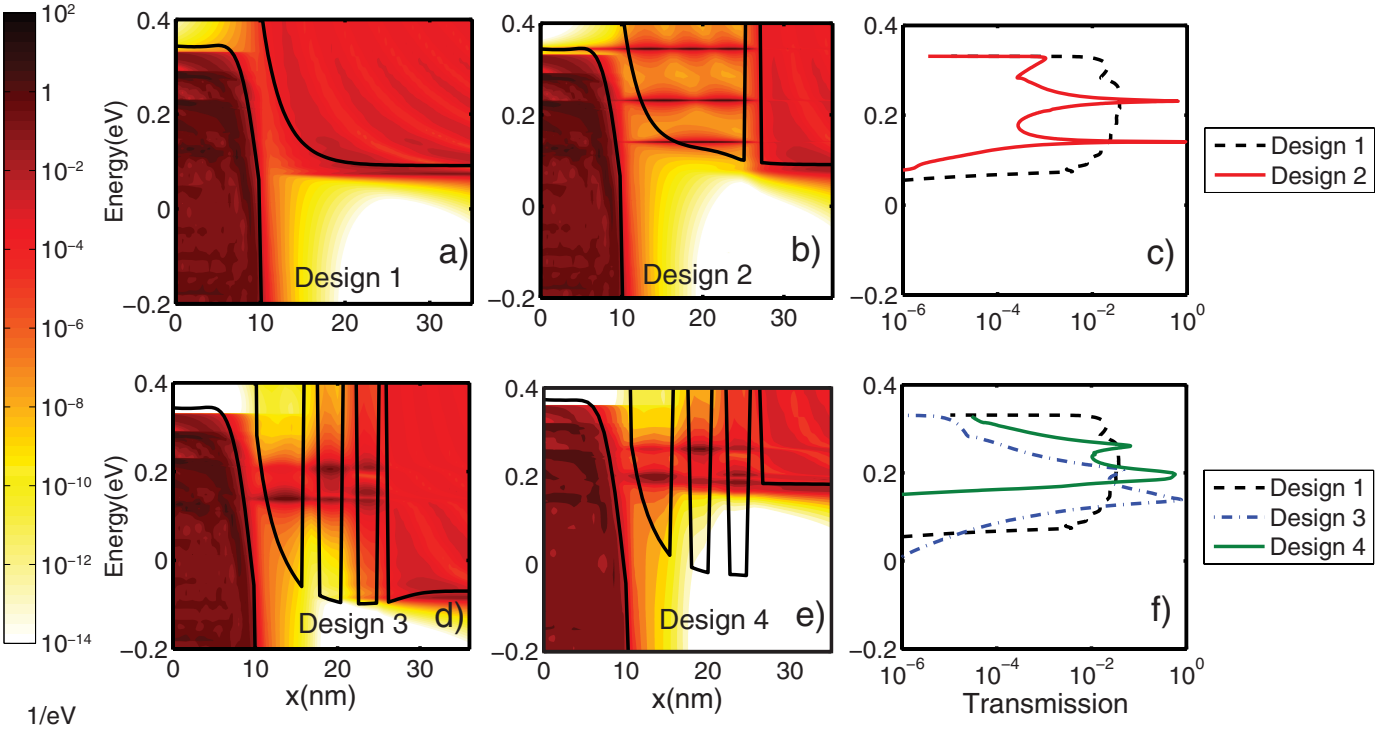

Fig. 2. Band diagram and energy-resolved LDOS at k_z=0 (in log scale) for Design 1 (a), Design 2 (b), Design 3 (d), and Design 4 (e); Comparison of transmission probabilities at k_z=0 for Design 1 and 2 (c), and for Design 3 and 4 (f). In all cases, ON state with V_{GS}=V_{DS} = 0.3V is assumed.

TABLE I
PARAMETERS FOR ONE-BARRIER AND THREE-BARRIER DESIGNS

Common Parameters		one-barrier		three-barrier	
		Region	Width (ml)	Region	Width (ml)
t_{ox}	2.56nm	w_1	49.5	w_2	18.5
$\varepsilon_{r,ox}$	20	b_1	6.5	b_2	6.5
t_{ch}	3.2nm			w_3	9.5
L_g	40nm			b_3	5.5
N_S	$5\cdot10^{19}$ cm^{-3}			w_4	9.5
N_D	$2\cdot10^{19}$ cm^{-3}			b_4	3

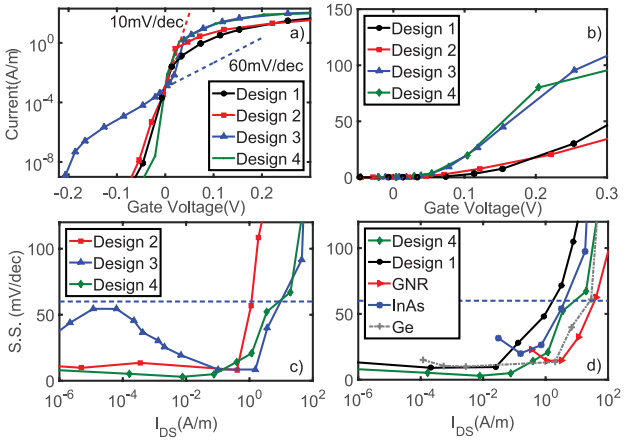

Fig. 3. a) Transfer characteristics of the four designs. The threshold voltage is adjusted for $I_{OFF} = 10^{-3}$A/m; b) linear scale of a); c) *S.S.* as a function of I_{DS} for Design 2, 3, and 4; d) *S.S.* as a function of I_{DS} for Design 1 and 4, compared with GNR, InAs, and Ge TFETs.

the Poisson equation and the open boundary Schrödinger equation (quantum transmitting boundary method [8], [9]). The band structure is described by tight binding model with sp^3d^5s* basis [10], [11]. Fig. 2a, b compare the band diagrams and the local densities of states (LDOS) of designs 1 and 2. Resonant states are formed in the quantum well of design 2; these increase the transmission from ∼4% (design 1) to ∼100% (design 2), (Fig. 2c). But, transmission is increased only in a narrow energy range around resonance. Design 3 has three closely aligned resonant states, (Fig. 2d), providing greater transmission over a broader energy range (Fig. 2f). The barrier and well widths have been adjusted to closely align the three states in energy, increasing transmission over a broad energy range.

In design 1, a normal TFET, subthreshold characteristics are determined by the relative energies of the source valence band and the channel conduction band. The subthreshold swing is consequently small (fig. 3a). In contrast, in designs 2 and 3, the subthreshold characteristics are determined by energy alignment between the source valence band and one or more resonant bound states. With design 3, these resonances are broad in energy (fig. 2f), and the *S.S.* is poorer (fig. 3a) than in design 1. For design 3, at gate-source biases at which the source valence band energy lies below the InAs channel conduction band energy, the subthreshold characteristics are set by energy filtering between the InAs channel conduction band and the GaSb source valence band. At such biases, the subthreshold characteristics are consequently very steep. At more positive gate biases, such that the source valence band energy lies above the InAs channel conduction band energy, the subthreshold characteristics are instead set by the energy-dependent transmission characteristics of the quantum wells.

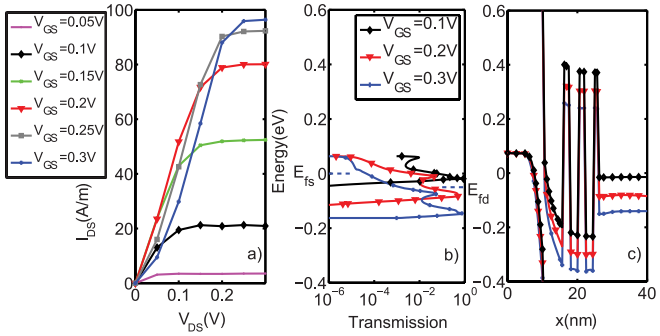

Fig. 4. Output characteristics (a), transmission probability at k_z=0 (b), and band diagram (c) of Design 4 for V_{GS}=0.3V, 0.2V, 0.1V.

At such biases, the subthreshold characteristics are consequently less steep. As the source Fermi energy approaches that of the resonant state, the slope of the transmission characteristics is steep, and consequently the *S.S.* is small. V_{DS} is set at 0.3V.

In design 4, the conduction band of the $In_{0.75}Ga_{0.25}As$ channel is aligned to the energy of the lowest resonant state (fig. 2e). The channel conduction band then causes (fig. 2f) the transmission below resonance to decrease rapidly with energy, and the subthreshold swing becomes small (fig. 3a). Note that, because the necessary tight-binding parameters were not available, the present simulations neglect the effect of strain upon the conduction-band energy of the $In_{0.75}Ga_{0.25}As$ channel. Given the effect of strain, $In_xGa_{1-x}As$ alloy fraction x and width of InAs wells must be adjusted to place the channel conduction band energy at the desired energy, slightly below that of the resonant states (fig. 2e). A detailed study including the effect of strain will be done in the future.

Comparing transfer characteristics computed with V_{th} adjusted for I_{off}=10^{-3}A/m (fig. 3a, b), design 1 has minimum *S.S.*=14.4mV/dec. and 35A/m I_{ON} at V_{DD}=0.3V. Design 2 has *S.S.*=8.7mV/dec. and a similar I_{ON}. Design 4 has both a small 4.6 mV/dec. *S.S.* and a large 96A/mI_{ON}. In designs 2 and 3, subthreshold characteristics are determined by resonant state transmission. In design 3, this resonant state has a broad energy range of transmission, thus the range of small S.S. is narrow (fig. 3c). Design 4 shows small *S.S.* over a wide current range (fig. 3d), broader even than that simulated (fig. 3d) with graphene nanoribbon (GNR) [12], InAs [13], and Ge [14] TFETs. Note, that in the present designs the gate length is large, being set by the length of the multi-barrier structure and of InGaAs channel. A minimum InGaAs channel length is required to suppress direct source-drain tunneling. It has been found recently that designs using two InAs wells and two AlSb barriers can provide similar on/off ratios at shorter gate lengths; these will be reported subsequently.

Fig. 4a shows common-source characteristics of design 4. At V_{DS} < 0.15V, I_{DS} first increases and then decreases with V_{GS}. This is a consequence (fig. 4b) of the transmission peak passing, as V_{GS} increases, through the energy range between the source E_f and drain E_f Fermi levels. The effect is present neither for V_{DS}>0.2V, nor for V_{GS} < 0.25V.

The effect of scattering has not been considered in this study. The effects of scattering on conventional III-V TFETs have been discussed in [15]–[17]: it is shown that phonon scattering slightly reduces I_{on}, but does not significantly degrade the subthreshold swing. In the transmission-enhanced TFET design 4, the *S.S.* is similarly determined by energy filtering between the channel conduction band and the source valence band, and consequently phonon scattering should not significantly degrade the subthreshold swing. In the transmission-enhanced TFET designs (2, 3, 4), carrier scattering, if sufficiently strong, will decreased the degree of resonant enhancement of the transmission, and will thus degrade I_{on}.

IV. Conclusion

Adding barriers within the channel of a TFET introduces reflected electron waves which destructively interfere with the reflections from the PN junction barrier, thereby increasing transmission. With multiple barriers, the transmission probability can be increased over a broad energy range, increasing the FET on-current.

Seeking to maximize the on-current, three-barrier design with the $In_{0.75}Ga_{0.25}As$ channel has its lowest resonant state aligned between the source and drain Fermi levels. Yet, the designs have many degrees of freedom and it is unlikely that an optimal design has been found by the present procedure of simulating a series of designs with varying well and barrier parameters. Known relationships between electron waves and electromagnetic filters [18], [19] suggest it may be possible to derive synthesis procedures for optimum design of electron matching layers.

Acknowledgment

The use of nanoHUB.org computational resources operated by the Network for Computational Nanotechnology funded by the U.S. National Science Foundation under Grant EEC-0228390, Grant EEC-1227110, Grant EEC-0634750, Grant OCI-0438246, Grant OCI-0832623, and Grant OCI-0721680 is gratefully acknowledged.

References

[1] T. N. Theis and P. M. Solomon, "In quest of the 'next switch': Prospects for greatly reduced power dissipation in a successor to the silicon field-effect transistor," *Proc. IEEE*, vol. 98, no. 12, pp. 2005–2014, Dec. 2010. DOI: 10.1109/JPROC.2010.2066531

[2] Q. Zhang, W. Zhao, and A. Seabaugh, "Low-subthreshold-swing tunnel transistors," *IEEE Electron Device Lett.*, vol. 27, no. 4, pp. 297–300, Apr. 2006. DOI: 10.1109/LED.2006.871855

[3] S. O. Koswatta, M. S. Lundstrom, and D. E. Nikonov, "Performance comparison between p-i-n tunneling transistors and conventional MOSFETs," *IEEE Trans. Electron Devices*, vol. 56, no. 3, pp. 456–465, Mar. 2009. DOI: 10.1109/TED.2008.2011934

[4] G. Dewey, B. Chu-Kung, J. Boardman, J. M. Fastenau, J. Kavalieros, R. Kotlyar, W. K. Liu, D. Lubyshev, M. Metz, N. Mukherjee, P. Oakey, R. Pillarisetty, M. Radosavljevic, H. W. Then, and R. Chau, "Fabrication, characterization, and physics of III–V heterojunction tunneling field effect transistors (H-TFET) for steep sub-threshold swing," in *Proc. IEEE Int. Electron Devices Meeting*, Dec. 2011, pp. 33.6.1–33.6.4. DOI: 10.1109/IEDM.2011.6131666

[5] M. J. W. Rodwell, C. Y. Huang, J. Rode, P. Choudhary, S. Lee, A. C. Gossard, P. Long, E. Wilson, S. Mehrotra, M. Povolotskyi, G. Klimeck, M. Urteaga, B. Brar, V. Chobpattanna, and S. Stemmer, "Transistors for VLSI, for wireless: A view forwards through fog," in *Proc. 73rd Annu. Device Res. Conf. (DRC)*, Jun. 2015, pp. 19–20. DOI: 10.1109/DRC.2015.7175529

[6] U. E. Avci and I. A. Young, "Heterojunction TFET scaling and resonant-TFET for steep subthreshold slope at sub-9 nm gate-length," in *Proc. IEEE Int. Electron Devices Meeting*, Dec. 2013, pp. 4.3.1–4.3.4. DOI: 10.1109/IEDM.2013.6724559

[7] J. E. Fonseca, T. Kubis, M. Povolotskyi, B. Novakovic, A. Ajoy, G. Hegde, H. Ilatikhameneh, Z. Jiang, P. Sengupta, Y. Tan, and G. Klimeck, "Efficient and realistic device modeling from atomic detail to the nanoscale," *J. Comput. Electron.*, vol. 12, no. 4, pp. 592–600, 2013. DOI: 10.1007/s10825-013-0509-0

[8] C. S. Lent and D. J. Kirkner, "The quantum transmitting boundary method," *J. Appl. Phys.*, vol. 67, no. 10, pp. 6353–6359, 1990. DOI: 10.1063/1.345156

[9] M. Luisier, A. Schenk, W. Fichtner, and G. Klimeck, "Atomistic simulation of nanowires in the $sp^3d^5s^*$ tight-binding formalism: From boundary conditions to strain calculations," *Phys. Rev. B*, vol. 74, no. 20, p. 205323. Nov. 2006. DOI: 10.1103/PhysRevB.74.205323

[10] T. B. Boykin, G. Klimeck, R. C. Bowen, and F. Oyafuso, "Diagonal parameter shifts due to nearest-neighbor displacements in empirical tight-binding theory," *Phys. Rev. B*, vol. 66, no. 12, p. 125207. Sep. 2002. DOI: 10.1103/PhysRevB.66.125207

[11] J.-M. Jancu, R. Scholz, F. Beltram, and F. Bassani, "Empirical spds* tight-binding calculation for cubic semiconductors: General method and material parameters," *Phys. Rev. B*, vol. 57, no. 12, p. 6493, Mar. 1998. DOI: 10.1103/PhysRevB.57.6493

[12] M. Luisier and G. Klimeck, "Performance analysis of statistical samples of graphene nanoribbon tunneling transistors with line edge roughness," *Appl. Phys. Lett.*, vol. 94, no. 22, p. 223505, Jun. 2009. DOI: 10.1063/1.3140505

[13] M. Luisier and G. Klimeck, "Atomistic full-band design study of InAs band-to-band tunneling field-effect transistors," *IEEE Electron Device Lett.*, vol. 30, no. 6, pp. 602–604, Jun. 2009. DOI: 10.1109/LED.2009.2020442

[14] A. Bowonder, P. Patel, K. Jeon, J. Oh, P. Majhi, H. H. Tseng, and C. Hu, "Low-voltage green transistor using ultra shallow junction and hetero-tunneling," in *Proc. 8th Int. Workshop Junction Technol.*, 2008, pp. 93–96. DOI: 10.1109/IWJT.2008.4540025

[15] M. Luisier and G. Klimeck, "Simulation of nanowire tunneling transistors: From the Wentzel–Kramers–Brillouin approximation to full-band phonon-assisted tunneling," *J. Appl. Phys.*, vol. 107, no. 8, p. 084507, 2010. DOI: 10.1063/1.3386521

[16] S. O. Koswatta, S. J. Koester, and W. Haensch, "On the possibility of obtaining MOSFET-like performance and sub-60-mV/dec swing in 1-D broken-gap tunnel transistors," *IEEE Trans. Electron Devices*, vol. 57, no. 12, pp. 3222–3230, Dec. 2010. DOI:10.1109/TED.2010.2079250

[17] U. E. Avci, D. H. Morris, S. Hasan, R. Kotlyar, R. Kim, R. Rios, D. E. Nikonov, and I. A. Young, "Energy efficiency comparison of nanowire heterojunction TFET and Si MOSFET at Lg = 13 nm, including P-TFET and variation considerations," in *Proc. IEEE Int. Electron Devices Meeting (IEDM)*, Dec. 2013, pp. 33.4.1–33.4.4. DOI: 10.1109/IEDM.2013.6724744

[18] A. N. Khondker, M. R. Khan, and A. F. M. Anwar, "Transmission line analogy of resonance tunneling phenomena: The generalized impedance concept," *J. Appl. Phys.*, vol. 63, no. 10, pp. 5191–5193, 1988. DOI: 10.1063/1.341154

[19] O. Vanbésien, H. Leroux, and D. Lippens, "Maximally flat transmission windows in finite superlattices," *Solid-State Electron.*, vol. 35, no. 5, pp. 665–669, 1992. DOI: 10.1016/0038-1101(92)90034-A